NEOPLASIA
www.neoplasia.com

Volume 14 Number 5 May 2012 pp. 440–450 **440**

BART Inhibits Pancreatic Cancer Cell Invasion by Rac1 Inactivation through Direct Binding to Active Rac1[1,2]

Keisuke Taniuchi*, Kunihiko Yokotani* and Toshiji Saibara†

*Department of Pharmacology, School of Medicine, Kochi University, Nankoku, Kochi, Japan; †Department of Gastroenterology and Hepatology, School of Medicine, Kochi University, Nankoku, Kochi, Japan

Abstract

We report that Binder of Arl Two (BART) plays a role in inhibiting cell invasion by regulating the activity of the Rho small guanosine triphosphatase protein Rac1 in pancreatic cancer cells. BART was originally identified as a binding partner of ADP-ribosylation factor-like 2, a small G protein implicated as a regulator of microtubule dynamics and folding. BART interacts with active forms of Rac1, and the BART-Rac1 complex localizes at the leading edges of migrating cancer cells. Suppression of BART increases active Rac1, thereby increasing cell invasion. Treatment of pancreatic cancer cells in which BART is stably knocked down with a Rac1 inhibitor decreases invasiveness. Thus, BART-dependent inhibition of cell invasion is likely associated with decreased active Rac1. Suppression of BART induces membrane ruffling and lamellipodial protrusion and increases peripheral actin structures in membrane ruffles at the edges of lamellipodia. The Rac1 inhibitor inhibits the lamellipodia formation that is stimulated by suppression of BART. Our results imply that BART regulates actin-cytoskeleton rearrangements at membrane ruffles through modulation of the activity of Rac1, which, in turn, inhibits pancreatic cancer cell invasion.

Neoplasia (2012) 14, 440–450

Introduction

BART is a soluble 19-kDa protein that was originally purified from bovine brain and identified as a binding partner of the small GTP-binding protein (G protein) ADP-ribosylation factor-like 2 (ARL2) [1]. Small G-ARL proteins lack the biochemical and genetic activities characteristic of the ADP-ribosylation factor family, despite the 40% to 60% amino acid sequence identity between ADP-ribosylation factors and ARLs [2]. ARL2 has been implicated as a regulator of microtubule dynamics and folding [3], but its function remains largely unknown. We previously reported that regulation of BART post-transcriptional modification through intracellular CD24 binding to G3BP in stress granules contributes to inhibition of invasion and metastasis of pancreatic ductal adenocarcinoma (PDAC) cells [4]. Further study demonstrated that BART decreases invasiveness of PDAC cells by inhibiting the ARL2-mediated decrease in the activity of the small guanosine triphosphatase (GTPase) protein RhoA [5]. The Rho family of GTPases cycle between an active guanosine 5′-triphosphate (GTP)–bound and inactive guanosine 5′-diphosphate (GDP)–bound state to control shape, motility, polarity, and behavior [6]. The Rho members, of which Rac1, Cdc42, and RhoA are the most commonly studied examples, play critical regulatory roles in several key cellular processes such as in the cytoskeletal rearrangement that underlies changes in cell shape, motility, and polarization [7,8]. Rac1 is activated by platelet-derived growth factor or insulin and induces the assembly of a meshwork of actin filaments at the cell periphery, producing lamellipodia and membrane ruffling; Cdc42 induces actin-rich surface protrusions or filopodia, whereas RhoA, which is activated by extracellular ligands, induces the assembly of contractile actin-myosin filaments (stress fibers) and associated focal adhesion complexes [9]. Migratory competence of tumor cells requires activation of the motile cycle, the first step of which is actin remodeling, which drives the formation of cell protrusions, defines the direction of migration, and initiates the growth of the lamellipodium [10]. Because

Address all correspondence to: Keisuke Taniuchi, MD, PhD, Department of Pharmacology, School of Medicine, Kochi University, Nankoku, Kochi 783-8505, Japan. E-mail: ktaniuchi@kochi-u.ac.jp

[1]This study was supported by a Grant-in-Aid for Scientific Research (KAKENHI) (to K.T.) and a Grant-in-Aid from the Ministry of Health, Labour and Welfare of Japan (to T.S.). The authors declare no competing financial interests.

[2]This article refers to supplementary material, which is designated by Figure W1 and is available online at www.neoplasia.com.

Received 15 February 2012; Revised 6 April 2012; Accepted 9 April 2012

DOI 10.1593/neo.12352

BART inhibits PDAC cell invasion by catalyzing GTP/GDP exchange of RhoA [5], it should be determined whether BART also functions in regulating the activity of other Rho GTPases.

Other evidence that BART is associated with the regulation of Rho GTPase activity has been reported. When BART interacts with ARL2, it affects the transcriptional activity and nuclear retention of signal transducer and activator of transcription 3 (STAT3), which is both a cytoplasmic signaling molecule and a nuclear transcription factor [11]. Recent studies have linked STAT3 to the metastatic progression of several different cancer types. Studies using mouse embryo fibroblasts established STAT3 as a component of the Rho GTPase signaling cascade [12,13]. Although the mechanisms that contribute to the constitutive activation of STAT3 in cancer invasion and metastasis are currently unclear, BART might contribute to the regulation of cell migration through the Rho GTPase signaling cascade.

In this study, we report the mechanism by which BART regulates the level of active Rac1 in PDAC cells. BART directly and predominantly binds to active forms of Rac1 and plays a role in decreasing the cellular level of active Rac1. BART and Rac1 are recruited to, and colocalize at, the leading edge of motile PDAC cells. Suppression of BART by RNA interference (RNAi) strongly enhances cell motility and invasiveness in PDAC cell systems [4]. The increased invasion resulting from BART knockdown was significantly abrogated by overexpression of BART, and treatment of BART RNAi cells with the Rac1 inhibitor decreased invasive activity. Thus, decreased levels of active Rac1 due to BART contributes to BART-mediated inhibition of invasion of PDAC cells. Further investigation suggested that BART regulation of Rac1 activity in PDAC cells inhibits cell invasion by restricting surface rearrangements of the actin cytoskeleton.

Materials and Methods

Reagents and Antibodies

The Rac1 inhibitor NSC23766 was obtained from Calbiochem (San Diego, CA). The RhoGAP Assay Biochem Kit was obtained from Cytoskeleton (Denver, CO). The rabbit anti-BART antibody (10090-2-AP) was purchased from ProteinTech (Chicago, IL). Monoclonal antibodies against Rac1 (610650), Cdc42 (610929), and β-catenin (610154) were obtained from BD Transduction Laboratory (Palo Alto, CA). Monoclonal antibody against RhoA (26C4) was purchased from Santa Cruz Biotechnology (Santa Cruz, CA). The rabbit anti–E-cadherin antibody (4065) was obtained from Cell Signaling (Danvers, MA). The rabbit anti-*myc* antibody (A14) was purchased from Santa Cruz Biotechnology.

Cell Culture

The human PDAC cell line S2-013, a subline of SUIT-2, was obtained from Dr T. Iwamura (Miyazaki Medical College, Miyazaki, Japan) [14]. The human PDAC cell line PANC-1 was obtained from the ATCC. Cells were grown in Dulbecco modified Eagle medium (Gibco-BRL, Carlsbad, CA) supplemented with 10% heat-inactivated fetal calf serum at 37°C in a humid atmosphere saturated with 5% CO_2.

Small Interfering RNA–Expressing Constructs and the Generation of Stable Cell Lines

The methods used were as previously reported [4].

Affinity Precipitation Using a Glutathione S-transferase–Fused Rac1 Interactive Binding Domain

The pGEX-6P1 plasmids encoding p21-activated kinase (PAK)–Cdc42/Rac interactive binding (CRIB) domain or Rhotekin were kindly provided by Dr K. Johnson (University of Nebraska Medical Center, Omaha, NE). Glutathione *S*-transferase (GST)–binding fusion proteins were purified from transformed *Escherichia coli* using glutathione-Sepharose beads and were used for affinity precipitation in GST-pull-down assays to estimate the activity of Rac1, Cdc42, and RhoA. Equal amounts of protein from each cell lysate that had been maintained in Dulbecco modified Eagle medium supplemented with 5% fetal bovine serum were incubated with 8 μg of GST-fusion protein, and the bound proteins were detected by Western blot analysis using anti-Rac1, anti-Cdc42, and anti-RhoA antibodies.

Wound Healing Motility Assay

A wound in the form of a cross was made through confluent cell monolayers with a plastic pipette tip. Several wound areas were marked for orientation and were then photographed under phase-contact microscopy. At set times ranging from 4 to 20 hours in individual experiments, marked wounds were photographed again, and the degree of wound closure was quantified. The number of cells that had migrated into the initially cell-free scratch area was counted.

Matrigel Invasion Assay

A two-chamber invasion assay was used to assess cell invasion (24-well plates, 8-μm pore size membrane coated with a layer of Matrigel extracellular matrix proteins; Becton Dickinson, Franklin Lakes, NJ). Cells (4.0×10^4) were seeded in serum-free medium into the upper chamber and allowed to invade toward a 5% fetal calf serum chemoattractant in the lower chamber. After 20 hours of incubation, the number of invading cells at the bottom of the membrane was estimated under microscopic observation by counting three independent visual fields.

In Vivo *Binding of BART with Rac1*

S2-013 cells were lysed in lysis buffer and immunoprecipitated with 2 μg of anti-BART or anti-Rac1 antibody. To examine the interaction of endogenous BART with endogenous Rac1, immune complexes were analyzed by Western blot analysis with anti-BART and anti-Rac1 antibodies.

Confocal Immunofluorescence Microscopy

Cells were fixed with 4% paraformaldehyde, permeabilized with 0.1% Triton X-100, covered with blocking solution (3% bovine serum albumin/phosphate-buffered saline), and then incubated with the primary antibody for 1 hour. Alexa 488 and Alexa 594–conjugated secondary antibodies (Molecular Probes, Carlsbad, CA) were used with or without rhodamine-conjugated phalloidin (Cytoskeleton). Each specimen was visualized using a Zeiss LSM 510 META microscope (Carl Zeiss, Gottingen, Germany). To investigate the functional link between BART and Rac1, 24 hours after transfection of *myc*-tagged BART-rescue plasmids into BART RNAi S2-013 cells, the cells were seeded on fibronectin-coated glass coverslips and incubated for 3 hours, followed by immunostaining with the indicated antibodies.

Wound Healing Immunostaining Assay

A wound in the form of a cross was made through the confluent cell monolayer with a plastic pipette tip, and the cells were then

allowed to polarize and migrate into the wound. After 4 hours, the cells were immunostained with the primary antibody and incubated with fluorophore-conjugated secondary antibodies as described above. Each specimen was visualized using a Zeiss LSM 510 META microscope.

Inhibition of Endogenous Rac1 by a Rac1-Specific Inhibitor

Cells cultured to 80% confluence were pretreated with the Rac1 inhibitor NSC23766 (100 μM) for 4 hours. After washing, the cells were analyzed by confocal immunostaining, GST-PAK-CRIB pull-down, Matrigel invasion, and wound healing assays.

Recombinant BART

The entire coding sequence of BART complementary DNA was amplified by reverse transcription–polymerase chain reaction. The product was subsequently inserted into the pIEx-7 Ek/LIC vector (Novagen, Madison, WI) to produce a fusion protein bearing an N-terminal 6-histidine tag. Sf9 cells (Novagen) were transiently transfected using the Insect GeneJuice Transfection Reagent (Novagen), according to the manufacturer's instructions. Transfected cells were lysed in CytoBuster Protein Extraction Reagent (Novagen) and centrifuged at 15,000*g* for 15 minutes. The supernatant was mixed with Ni-NTA His-Bind Resin (Novagen), and the bound proteins were eluted. Western blot analysis using an anti-BART antibody was performed to identify the fractions containing BART. The fractions corresponding to apparently pure proteins were pooled and dialyzed against storage buffer consisting of 20 mM HEPES (pH 7.4), 20 mM KCl, and 10% glycerol. The samples were stored at −80°C.

GST-Rac1 Binding Assay In Vitro

GST-tagged Rac1 protein (8 μg) attached to glutathione-agarose beads (Cytoskeleton) was incubated either with GTPγS or with GDP at a final concentration of 1 mM in 20 μl of reaction buffer (50 mM HEPES [pH 7.4], 100 mM NaCl, 10 mM $MgCl_2$, 5 mM EDTA, 1 mM DTT) at 30°C for 15 minutes. The $MgCl_2$ concentration of the buffer was then increased to 50 mM. and 6 μg of recombinant BART protein was added and incubated at 4°C for 4 hours. GST was used as a control. After the beads were extensively washed with lysis buffer, the bound proteins were detected by Western blot analysis using anti-BART and anti-Rac1 antibodies.

GST-Rac1/Rac1N17 Pull-down Assays Using PDAC Cell Lysates

GST-Rac1 and -Rac1N17 proteins attached to glutathione-agarose beads were obtained from Cytoskeleton. S2-013 cells were lysed in lysis buffer, and equal amounts of total lysates were incubated with 8 μg of each GST-fusion protein at 4°C for 1 hour. GST was used as a control. Western blot analysis with anti-BART antibody was performed to detect coprecipitated BART.

BART-Rescue Construct

The entire coding sequence of the BART complementary DNA was amplified using reverse transcription–polymerase chain reaction. The product was subsequently inserted into a pCMV6-Entry vector (Origene, Rockville, MD) bearing a C-terminal *myc*-DDK-tag. This BART-rescue construct was transiently transfected into cells using FuGENE6 (Roche, Penzberg, Germany).

In Vitro *Rho–GTPase-Activating Protein Assay*

In vitro GTPase-activating protein (GAP) assays were performed in triplicate using the RhoGAP Assay Biochem Kit (Cytoskeleton). His-tagged Rac1 (5 μg; Cytoskeleton) was incubated with recombinant BART protein (0.5 μmol) and 200 μM GTP with or without the p50 RhoGAP protein (0.5 μmol; Cytoskeleton) at 37°C for 20 minutes in a reaction mixture (20 μl) containing 25 mM HEPES (pH 7.4), 100 mM NaCl, 2 mM $MgCl_2$, and 1 mM DTT. GST protein (0.5 μmol) was used as a negative control for BART. Phosphate generated by hydrolysis of GTP was measured by adding the CytoPhos reagent (Cytoskeleton), and the absorbance was read at 650 nm.

Cytosol and Membrane Fractionation

Cells were homogenized in hypotonic buffer (20 mM Tris-HCl [pH 8.0], 150 mM NaCl, 1 mM EDTA, 1 mM phenylmethylsulfonyl fluoride, and 1 mM Na_3VO_4) using a Dounce homogenizer and centrifuged at 700*g* for 5 minutes, and the postnuclear supernatant was then centrifuged at 100,000*g* for 1 hour. The resulting supernatant was collected and used as the cytosolic fraction. The pellet was resuspended in hypotonic buffer containing 1% Triton X-100 and incubated on ice for 1 hour. The supernatant component (particulate fraction) was centrifuged at 14,000*g* for 20 minutes. Protein concentrations were determined with the Bio-Rad protein assay (Hercules, CA) using bovine serum albumin as a standard.

Statistical Analysis

The significance of differences between groups was determined using Student's *t* test, the Mann-Whitney *U* test, or Fisher exact test, as appropriate. $P < .05$ was considered statistically significant.

Results

BART Decreases the Level of Active Rac1 and Inhibits PDAC Cell Motility and Invasion

BART expression is suppressed by a vector-based specific short hairpin small interfering RNA (siRNA) in the PDAC cell lines S2-013 and PANC-1 that express high levels of endogenous BART [4]. Knockdown of BART increases retroperitoneal invasion and liver metastasis of PDAC cells in an orthotopic xenograft model [4]. To determine the effect of BART depletion on Rac1 activity, we assayed Rac1 activity of cell lysates by performing a GST-pull-down assay using a GST-Rac1 interactive binding domain fusion protein (GST-PAK-CRIB; Figure 1*A*). We found that suppression of BART resulted in an increase in active Rac1 compared with mock-transfected or scrambled siRNA-transfected cells, suggesting that endogenous BART is associated with a decrease in the activity of Rac1. The amount of GTP-Cdc42, a closely related Rho GTPase, was not affected (data not shown). We next determined the effect of the Rac1 inhibitor NSC23766 [15] on the cell motility and invasion of control and BART RNAi S2-013 cells. We confirmed that pretreatment of BART RNAi-S2-013 cells with the Rac1 inhibitor decreased the level of GTP-Rac1 (Figure 1*B*). The amounts of GTP-Cdc42 and GTP-RhoA were not affected (Figure 1*B*), confirming the specificity of NSC23766. Pretreatment of control and BART RNAi S2-013 cells with the Rac1 inhibitor significantly inhibited cell motility in a wound healing assay and Matrigel invasion in a two-chamber assay (Figure 1, *C* and *D*, respectively). Importantly, the Rac1 inhibitor decreased cell motility and invasiveness of BART RNAi S2-013 cells to the levels of the control cells that had not been pretreated with the Rac1 inhibitor (Figure 1,

C and *D*). These results indicate that activated Rac1 plays an important role in accelerating cell migration and that BART-dependent inhibition of PDAC cell motility, and invasion is likely to be associated with a decrease in active Rac1.

BART Binds to Rac1 at Cell Protrusions

To determine whether BART and Rac1 associate in PDAC cells, endogenous BART and Rac1 were immunoprecipitated from S2-013 cells, followed by immunoblot analysis using anti-BART and anti-Rac1 antibodies (Figure 2*A*). This experiment indicated that BART did coimmunoprecipitate with Rac1 from S2-013 cells. We next examined the subcellular localization of BART and Rac1 in S2-013 cells using immunofluorescence (Figure 2*B*). BART and Rac1 colocalized in both the cytoplasm and in lamellipodial-like protrusions. The latter localization is characteristic of factors that modulate, and are essential for, cell migration (Figure 2*B*, *arrows*). Rac1, Cdc42, and RhoA are best known as master regulators of the actin cytoskeleton and promote the formation of lamellipodia, filopodia, and stress fibers, respectively [6]. We therefore hypothesized that BART is associated with the regulation of lamellipodia formation through a decrease in the activity of Rac1 and thereby inhibits cell invasion. In addition, the localization of BART and Rac1 in polarized migrating

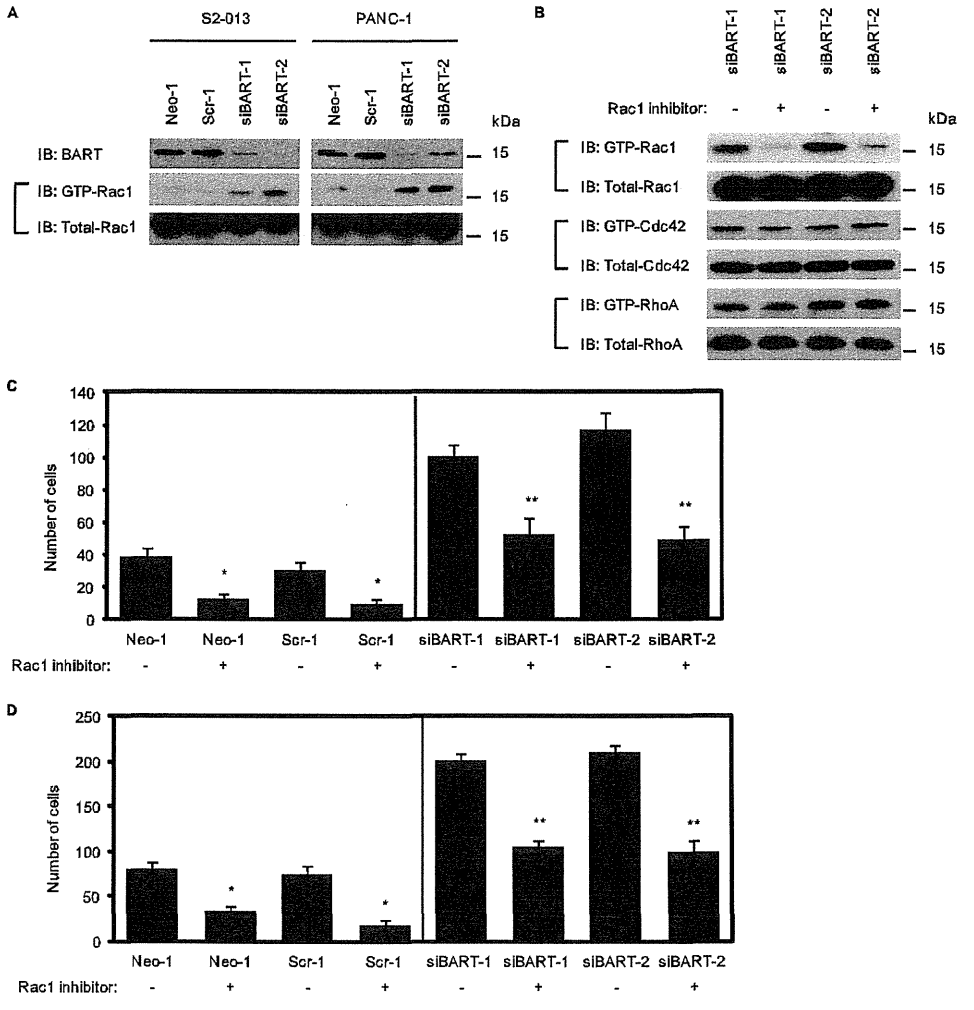

Figure 1. BART decreases the activity of Rac1 resulting in inhibition of PDAC cell motility and invasion. (A) The amount of active, GTP-loaded Rac1 in S2-013 and PANC-1 cells that were mock transfected (Neo-1) or transfected with control, scrambled (Scr-1), or BART (siBART-1 and 2) siRNA was determined using a GST-PAK-CRIB pull-down assay. Precipitates were examined by Western blot analysis using an anti-Rac1 antibody. Data are representative of three independent experiments. (B) Two S2-013 clones transfected with siRNA for BART were pretreated with or without the Rac1 inhibitor (NSC23766), and the amount of active GTP-loaded Rac1 and Cdc42 and RhoA was analyzed with GST pull-down assays using GST-PAK-CRIB and GST-Rhotekin, respectively. Precipitates were examined by Western blot analysis using anti-Rac1, anti-Cdc42, and anti-RhoA antibodies. Total levels of Rac1, Cdc42, and RhoA protein were used to normalize the data. Data are representative of three independent experiments. (C) Confluent control and BART RNAi S2-013 cells treated as in B were wounded. The number of cells that migrated into an initially cell-free scratch was counted. Cells in four defined areas per group per experiment were quantified. Data are representative of three independent experiments. Bars, SD; columns, mean. $^{*}P < .005$, $^{**}P < .001$ compared with nontreated cells. (D) Control and BART RNAi S2-013 cells treated as in B were plated on Matrigel invasion chambers. Invaded cells in four fields per group were counted. Data are representative of three independent experiments. Bars, SD; columns, mean. $^{*}P < .005$, $^{**}P < .001$ compared with nontreated cells.

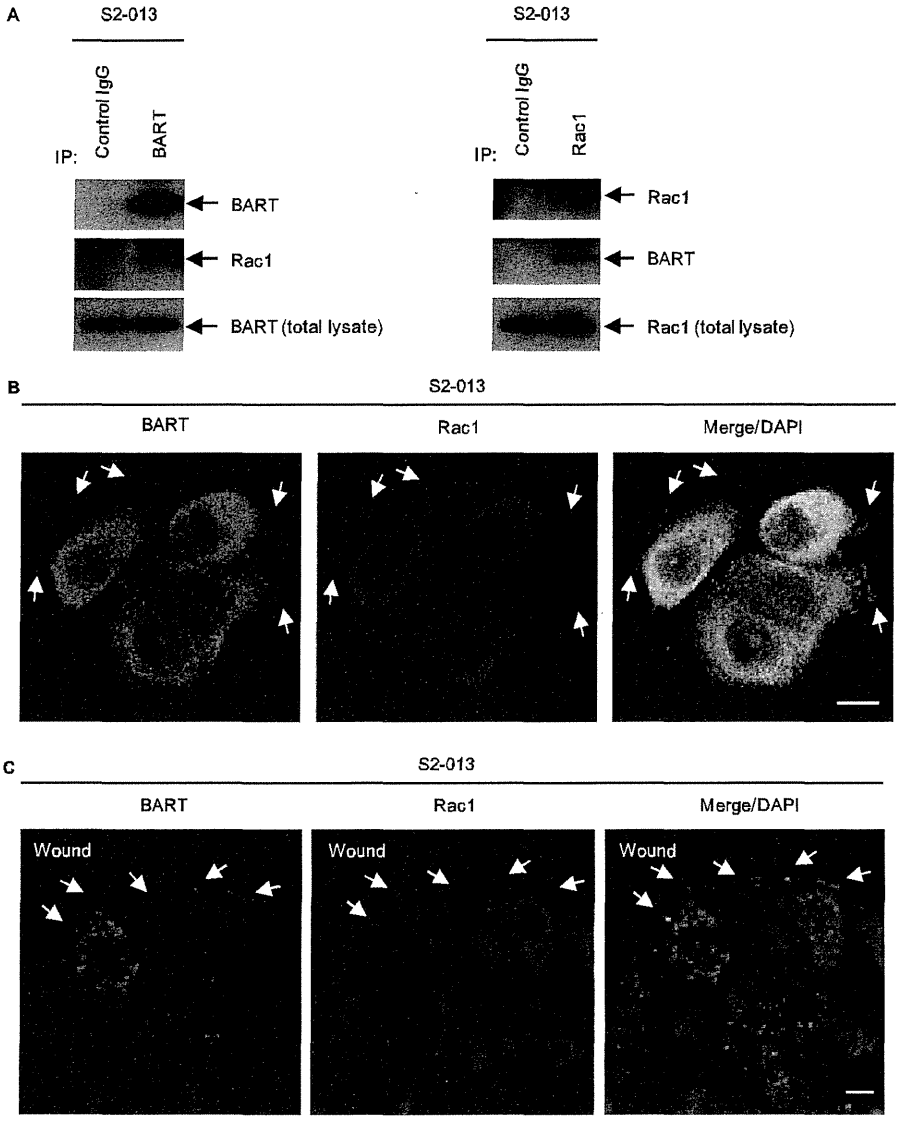

Figure 2. BART binds to Rac1 at the leading edges of migrating cells. (A) Immunoprecipitation of endogenous BART or Rac1 from S2-013 cells. Anti-BART or anti-Rac1 immunoprecipitates were examined by Western blot analysis using anti-BART and anti-Rac1 antibodies. Rabbit IgG and mouse IgG monoclonal antibodies were used as isotype controls for anti-BART and anti-Rac1 antibodies, respectively. Data are representative of three independent experiments. (B) Immunocytochemical staining of S2-013 cells using anti-BART (green) and anti-Rac1 (red) antibodies. Arrow indicates colocalized BART and Rac1 in lamellipodial-like protrusions; blue, DAPI staining. Bar, 10 μm. (C) Confluent S2-013 cells were wounded. After 4 hours, the cells were immunostained using anti-BART (green) and anti-Rac1 (red) antibodies. Arrows indicate colocalized BART and Rac1 at the leading edge; blue, DAPI staining. Bar, 10 μm.

S2-013 cells was analyzed using a wound healing immunostaining assay (Figure 2*C*). This assay showed that BART and Rac1 were recruited to the leading edges during wound healing of S2-013 cells, indicating that they function interdependently in cell migration.

Cell-cell adhesion can also influence cell motility [16]. On the formation of cell-cell contacts, cells reduce their migration rate and cell surface protrusion activity and decrease their microtubule and actin-filament dynamics [17]. Rac has been shown to be important both upstream and downstream of adherens junction formation, and too much or too little Rac activity disrupts adherens junctions in cultured mammalian epithelial cells [18–20]. To determine the effect of Rac1 on cell-cell contact, S2-013 cells were incubated with the Rac1 inhibitor NSC23766, and adherens junctions were analyzed by immunofluorescence using anti–E-cadherin and anti–β-catenin antibodies (Figure W1*A*). We found that the Rac1 inhibitor did not affect the presence of these junction proteins at regions of cell-cell contact of S2-013 cells. However, interestingly, the level of these junction proteins at the cell-cell contacts of S2-013 cells was significantly reduced in BART RNAi cells compared with control cells (Figure W1*B*), indicating a decreased peripheral localization of junction proteins in these cells that resulted in adherens junctions with decreased stability. These results suggest that, although BART plays a role in inhibiting cell invasion through decreasing active Rac1 and colocalizes with Rac1 at the leading edges of migrating cells, BART also functions in regulation of the

stability of cell-cell contacts in a Rac1-independent manner. The mechanism by which BART influences cell-cell contacts is still unknown.

BART Binds to an Active Form of Rac1

To determine the activation state of the Rac1 that binds to BART, GST-tagged Rac1 was incubated with GDP or GTPγS and then used in *in vitro* pull-down experiments with the recombinant BART protein (Figure 3*A*). A significant amount of the constitutively active GTPγS-Rac1 bound to BART compared with the inactive GDP-Rac1 form, which only weakly interacted with BART. Further pull-down experiments were carried out to confirm this interaction in PDAC cells (Figure 3, *B* and *C*). Binding of endogenous BART to GST-tagged wild-type Rac1, a dominant-negative mutant Rac1 form, Rac1N17, or the CRIB motif that interacts with GTP-Rac1, was assayed by incubation of these GST proteins with S2-013 cell lysates, followed by a GST-pull-down assay and Western blot analysis with

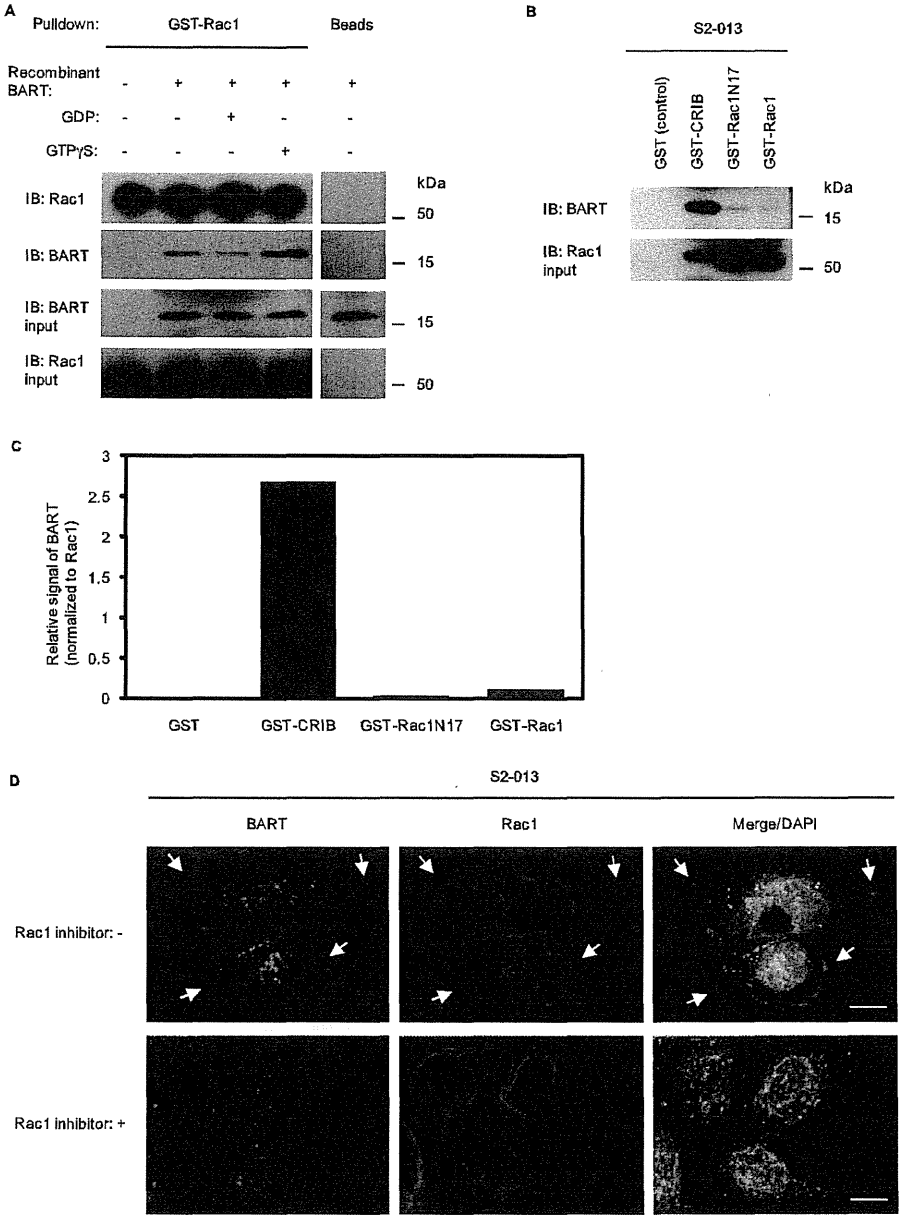

Figure 3. BART binds to an active form of Rac1. (A) GST-tagged Rac1 was incubated with GDP or GTPγS and was then used in pull-down experiments with the recombinant BART protein. Precipitates were examined by Western blot analysis using anti-BART and anti-Rac1 antibodies. Data are representative of three independent experiments. (B) GST-tagged Rac1, a dominant-negative mutated Rac1 form, Rac1N17, or PAK-CRIB was incubated with S2-013 cell lysates, followed by GST-pull-down assays. Precipitates were examined by Western blot analysis using anti-BART and anti-Rac1 antibodies. Data are representative of three independent experiments. (C) Densitometric analysis of the results of B. The level of BART in the precipitates was assessed after normalizing BART signals to Rac1 signals. (D) S2-013 cells were pretreated with or without the Rac1 inhibitor (NSC23766) and were immunocytochemically stained using anti-BART (green) and anti-Rac1 (red) antibodies. Arrows indicate colocalized BART and Rac1 in lamellipodial-like protrusions; blue, DAPI staining. Bars, 10 μm.

anti-BART and anti-Rac1 antibodies. The CRIB motif has been found only in effectors for Rac1 but not in RhoGAPs [21]. The interaction of GST-tagged CRIB with endogenous BART in S2-013 cells through GTP-bound Rac1 was significantly higher than that of wild-type Rac1 or Rac1N17. In the immunocytochemical analysis of S2-013 cells, BART and Rac1 colocalized in lamellipodial-like protrusions in the absence of treatment with the Rac1 inhibitor NSC23766 (arrows in Figure 3*D*). Treatment of S2-013 cells with NSC23766 led to inhibition of membrane ruffling and decreased the binding of BART with Rac1 (Figure 3*D*). These results suggest that BART preferentially binds to the active GTP-Rac1 in cell protrusions.

BART Has GAP Activity toward Rac1

To investigate the functional link between BART and Rac1, we assessed the effect of BART on the regulation of Rac1 activity using BART RNAi-S2-013 cells that expressed the BART-rescue construct. Expression of this construct was confirmed by Western blot analysis (Figure 4*A*). The increased activity of Rac1 that resulted from BART knockdown was significantly abrogated by overexpression of BART in BART RNAi clones. This result confirmed the data shown in Figure 1*A*. We therefore hypothesized that Rac1 might be a direct substrate of BART. RhoGAPs stimulate the low intrinsic GTPase activity of Rho GTPase proteins, leading to conversion of GTP-bound active forms of Rho GTPases to GDP-bound inactive forms. To determine whether BART has GAP function toward Rac1, we performed *in vitro* GAP assays using the recombinant BART protein (Figure 4*B*). We previously demonstrated that ARL2 markedly increased the GTPase activity of RhoA by using this system [5]. Recombinant BART and human Rac1 GTPase were incubated with or without the human p50 RhoGAP protein. The GAP domain of p50 RhoGAP is known to stimulate the GTPase activities of Rac1 *in vitro*. In these studies, BART significantly increased the GTPase activity of Rac1 to the same extent as p50 RhoGAP, but this effect of BART was not associated with an effect on the GAP activity of p50 RhoGAP toward Rac1 (Figure 4*B*). These results suggest that BART plays a role in inactivating Rac1 by acting as a GAP toward Rac1 and that Rac1 may be a preferred substrate of BART.

BART Inhibits the Translocation of Rac1 to the Plasma Membrane

Like other members of the Ras small GTPase family, Rho proteins function as molecular switches that transduce extracellular stimuli into intracellular responses and that cycle between a soluble, GDP-bound inactive state and a membrane-associated GTP-bound active state [22]. We analyzed the subcellular distribution of Rac1 in BART RNAi S2-013 cells cultured on fibronectin after transfection of the BART-rescue construct. Adhesion of cells to fibronectin induces the assembly of focal adhesion complexes that are linked to the actin cytoskeleton [23]. Rac1 is known to contribute to the regulation of corneal epithelial cell adhesion or migration on fibronectin [24]. We found that transfection of a BART-rescue construct inhibited fibronectin-stimulated Rac1 activation in BART RNAi cells (Figure 5*A*). Because translocation of Rac1 from the cytosol to the cytoplasmic membrane is required for its activation and functions, the effect of BART on Rac1 membrane translocation was investigated by analyzing subcellular fractionations of BART RNAi S2-013 cells transfected with the BART-rescue construct and cultured on fibronectin (Figure 5*B*). Transfection of the BART-rescue construct significantly reduced fibronectin-stimulated Rac1 in the particulate fraction of the BART RNAi cells. Incubation on fibronectin did not increase active Rac1 in the particulate fraction of the control cells, and control cells transfected with the BART-rescue construct did not show any significant changes (Figure 5*B*). Immunocytochemical analysis showed that Rac1 was translocated to the plasma membrane in BART RNAi cells, whereas in cells expressing the BART-rescue construct, Rac1 was mainly located in the cytoplasm and only a little Rac1 was seen at the cell membrane (Figure 5*C*). After transfection with the mock plasmid, Rac1 was more abundantly expressed in the cytoplasm of control cells than the BART RNAi cells, and the BART-rescue construct did not change the intracellular localization of Rac1 (Figure 5*C*). Accordingly, these results provide supportive

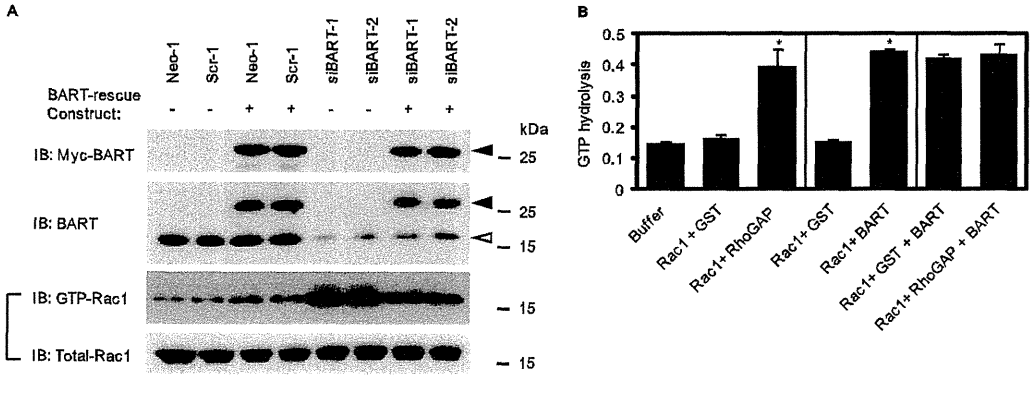

Figure 4. BART has GAP activity toward Rac1. (A) The BART-rescue construct was transfected into control and BART knockdown cells of S2-013, and 48 hours later, the amount of active GTP-loaded Rac1 was determined by GST-pull-down assays using GST-PAK-CRIB. Precipitates were examined by Western blot analysis using an anti-Rac1 antibody. Data are representative of three independent experiments. Closed arrowhead indicates exogenous BART; open arrowhead, endogenous BART. (B) The possibility that BART might have a GAP function for Rac1 GTPase was assayed by *in vitro* GAP assays using human Rac1 with or without the human p50 RhoGAP protein together with recombinant BART protein. GST was used as a negative control for RhoGAP and BART protein. GAP activity was assayed by measurement of the phosphate generated by hydrolysis of GTP. Data are representative of three independent experiments and are shown as means ± SEM. *$P < .005$ compared with their respective controls.

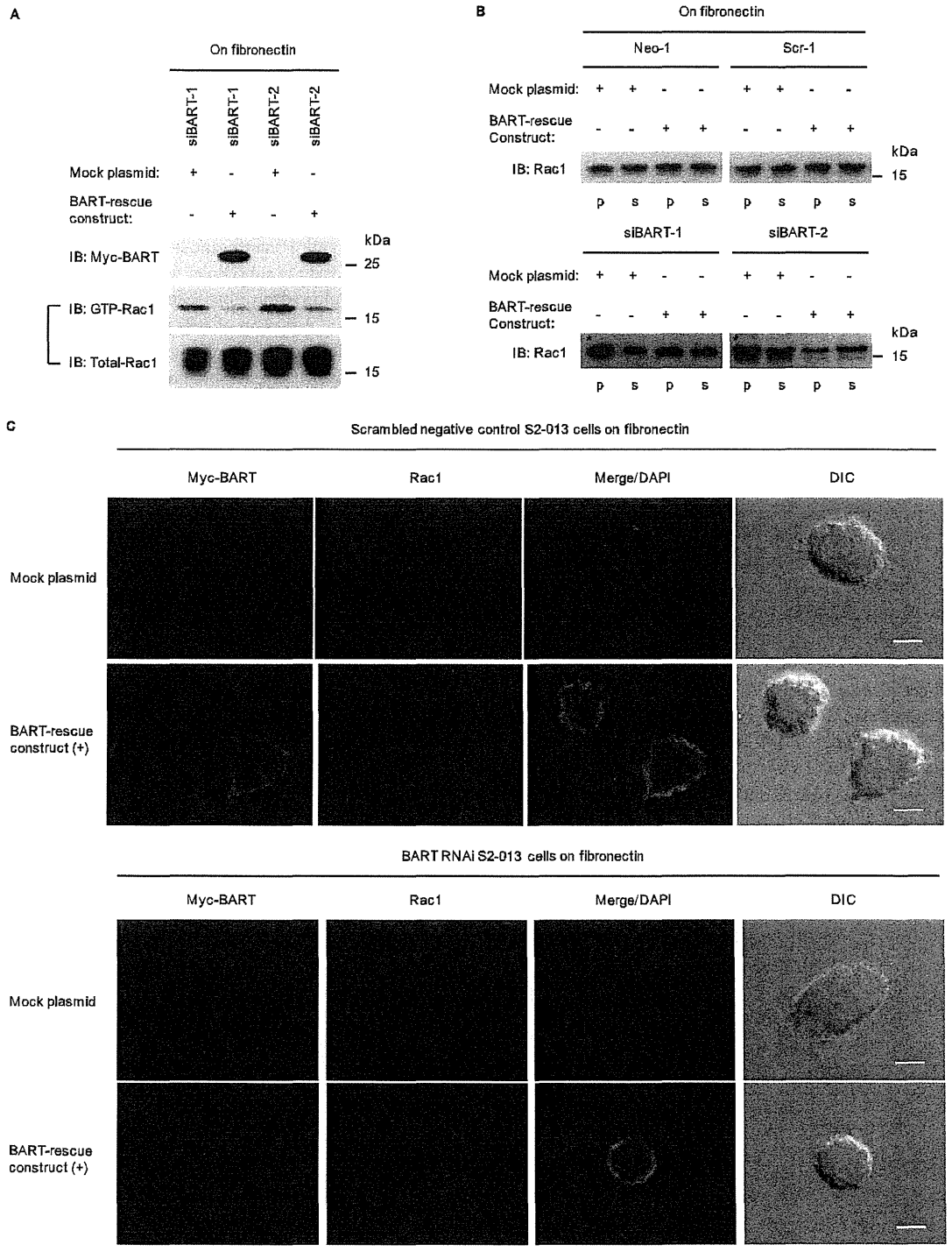

Figure 5. BART inhibits the translocation of Rac1 to the plasma membrane. (A) The mock control vector or *myc*-tagged BART-rescue construct was transfected into BART knockdown cells of S2-013, and 48 hours later, the cells were incubated on fibronectin for 1 hour. GST-pull-down assays were performed using GST-PAK-CRIB. The precipitates were immunoblotted with anti-*myc* and anti-Rac1 antibodies. Data are representative of three independent experiments. (B) Control (Neo-1 and Scr-1) and BART RNAi (siBART-1 and 2) S2-013 cells treated as in A were fractionated, and particulate/membranous (p) and soluble/cytosolic (s) fractions were analyzed by Western blot using anti-Rac1 antibody. Asterisk indicates fibronectin-stimulated Rac1 in the particulate fraction of BART RNAi cells. Data are representative of three independent experiments. (C) Scrambled control (Scr-1) and BART RNAi (siBART-1) S2-013 cells treated as in A were immunocytochemically stained using anti-Rac1 (green) and anti-*myc* (red) antibodies. Blue indicates DAPI staining. The corresponding differential interference contrast (DIC) images are shown. Bars, 10 μm.

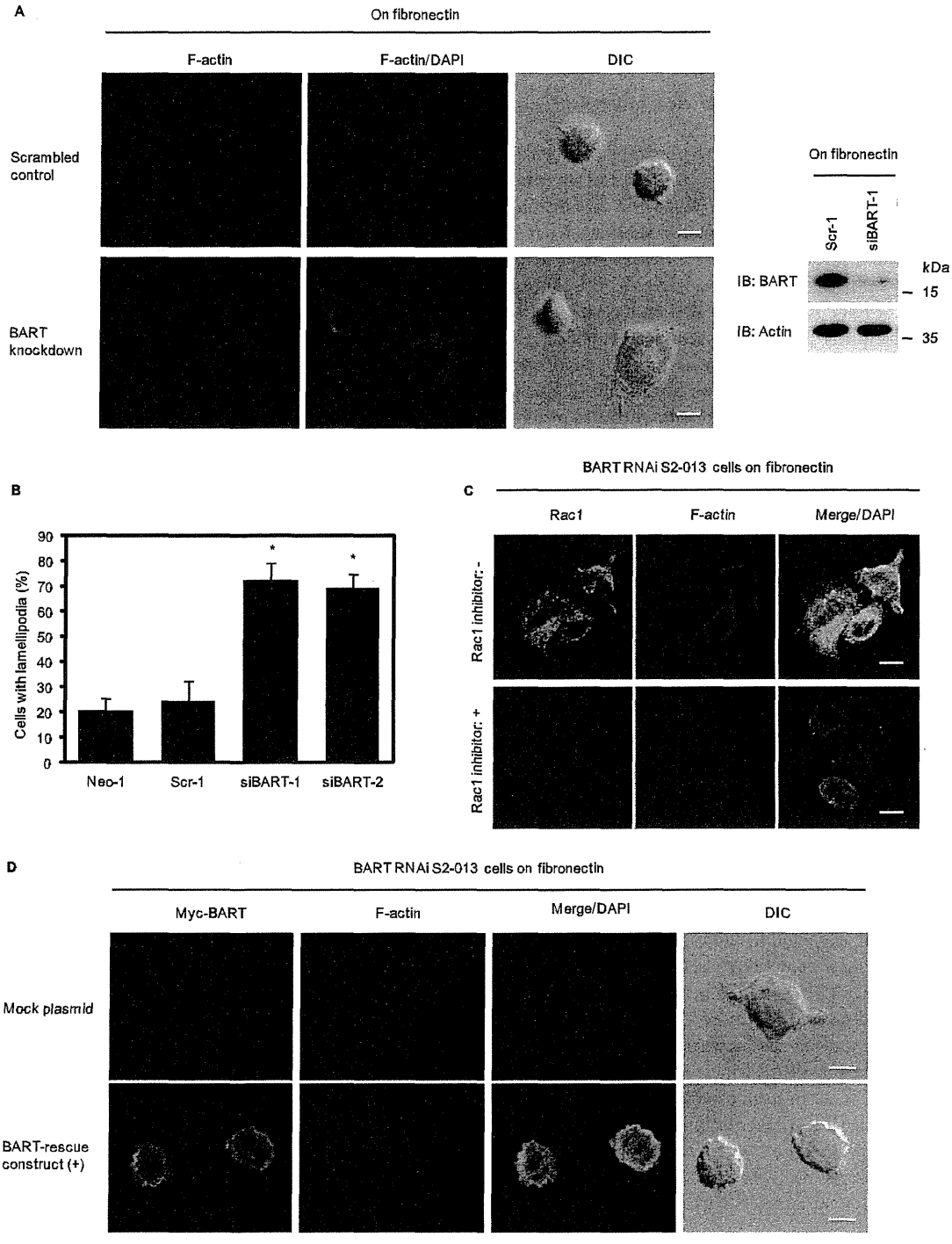

Figure 6. BART inhibits membrane lamellipodial formation by inhibiting peripheral actin-cytoskeletal rearrangements. (A) Scrambled control (Scr-1) and BART knockdown (siBART-1) S2-013 cells were incubated on fibronectin for 1 hour, and then actin was immunocytochemically stained using phalloidin (red) (left panels). Blue indicates DAPI staining. The corresponding DIC images are shown. Bars, 10 μm. Western blot with anti-BART antibody showing the siBART-1 cells compared with the control Scr-1 cells incubated on fibronectin (right panels). (B) Quantification of data shown in A; the values represent the number of scrambled control and BART knockdown S2-013 cells with lamellipodial protrusion. Cells in four fields per group were counted. Data are representative of three independent experiments. Bars, SD; columns, mean. *P < .005 compared with control cells. (C) BART RNAi S2-013 cells (siBART-1) were pretreated with or without the Rac1 inhibitor (NSC23766) and then incubated on fibronectin for 1 hour. The cells were immunocytochemically stained using anti-Rac1 antibody (green), and cellular actin was then stained using phalloidin (red). Blue indicates DAPI staining. Bars, 10 μm. (D) The mock control vector or BART-rescue construct was transfected into BART knockdown S2-013 cells (siBART-1), and 48 hours later, the cells were incubated on fibronectin for 1 hour. The cells were immunocytochemically stained using anti-*myc* antibody (green), and cellular actin was then stained using phalloidin (red). Blue indicates DAPI staining. The corresponding DIC images are shown. Bars, 10 μm.

evidence that BART decreases active Rac1 and thereby inhibits the translocation of Rac1 to the plasma membrane.

BART Inhibits Peripheral Cytoskeletal Rearrangements of Actin

Rac1, Cdc42, and RhoA are important regulators of actin dynamics and cell-substratum adhesions in migratory cells and thus are critically involved in cell motility and invasion [25]. When cells that are initially suspended adhere to an immobilized fibronectin substrate, a temporal wave of Rac1 activation is induced, which correlates with the initial membrane protrusion observed during spreading [26]. Cell shrinkage–induced activation of Rac1 results in the *de novo* formation of actin patches at the cell periphery [27,28]. We analyzed peripheral F-actin structures in membrane ruffles at the edge of lamellipodia of control and BART RNAi S2-013 cells cultured on fibronectin (Figure 6, *A* and *B*). Suppression of BART induced fibronectin-mediated membrane ruffles and lamellipodial protrusions in S2-013 cells. To evaluate the ability of Rac1 to induce such membrane ruffles, we next examined the actin cytoskeleton structures of BART RNAi S2-013 cells on fibronectin in the absence or presence of the Rac1 inhibitor NSC23766 (Figure 6*C*). Suppression of BART induced surface rearrangements of the actin cytoskeleton, and NSC23766 inhibited these surface actin rearrangements that were stimulated by suppression of BART. In addition, transfection of the BART-rescue construct into BART RNAi S2-013 cells also reduced these peripheral actin rearrangements (Figure 6*D*). These results indicate that BART plays a role in inhibiting peripheral actin-cytoskeletal rearrangements through decreasing active Rac1.

Discussion

PDAC is one of the deadliest cancers owing to its ability to extensively invade surrounding tissues and metastasize at an early stage [29]. Extensive local infiltration and metastasis are the main causes of death in PDAC [30]. Here, we report a novel function for BART in the regulation of cell migration in PDAC. The invasive activity of stably BART siRNA-transfected PDAC cells was inhibited by pretreatment with the specific Rac1 inhibitor NSC23766 *in vitro* (Figure 1, *C* and *D*). The decreased activity of Rac1 inhibits cell invasion and is required for the anti-invasive activity of BART.

We previously reported that BART increases active RhoA by inhibiting ARL2 function, which, in turn, inhibits the invasive activity of cancer cells [5]. The BART-ARL2 complex interacts with RhoA; ARL2, and not BART, possesses GAP activity toward RhoA [5]. However, ARL2 did not interact with the BART-Rac1 complex (data not shown). BART directly interacts with GTP-bound Rac1 (Figure 3, *A-D*) to decrease Rac1 activity (Figure 4*B*), indicating that BART does not require ARL2 association to regulate Rac1 activity. Our data suggest that BART inactivates Rac1 by acting as a GAP, and that Rac1 may be a preferred substrate for BART. It is hypothesized that the active sites of many different GAPs contain an arginine finger [31]. ARL2, which has a conserved arginine residue, regulates the tubulin-GAP activity of cofactors C and D, which, in turn, affects microtubule stability [32]. Because no GTPase activity–triggering arginine finger residue has been found in BART, further studies are needed to determine the structure and binding site of BART for the active forms of Rac1; this will enable understanding of the mechanism by which the BART-Rac1 complex, which is essential for cell migration, is formed at the leading edge of migrating cells.

Several lines of evidence indicate that Rac1 may play critical roles in several aspects of tumorigenesis and cancer progression. Loss of function of PTEN, $p19^{Arf}$, or the p53 tumor suppressor leads to elevation of Rac1 activity, resulting in increased migration and proliferation in $PTEN^{-/-}$, $p19^{Arf-/-}$, or $p53^{-/-}$ cells [33–35]. K-*ras* is mutated to an oncogenic, active GTPase form in most PDAC, and K-*ras* is known to signal through Rac1 in some cell types [36]. Unlike Ras, however, constitutively active mutation of Rac1 has not been found in human cancer [15]. Rho GTPases function as molecular switches that shuttle between an active GTP-bound state and an inactive GDP-bound state, which can form a complex with GDI (guanosine nucleotide dissociation inhibitor) proteins [37]. GTPase activation requires dissociation from GDIs and exchange of GDP for GTP and is catalyzed by guanosine nucleotide exchange factors that are activated by upstream signaling events [38]. Therefore, the signaling step of Rac1 activation by a guanosine nucleotide exchange factor could be a target site of signaling cascades that involve Rac1. GTPases are turned off by intrinsic GTP hydrolysis, which is enhanced by interaction with GAPs [38]. We found that BART directly stimulates the GTPase activity of Rac1 (Figure 4*B*), which, in turn, constitutively inactivates Rac1 (Figures 4*A* and 5, *A-C*). Our data suggest that the GAP activity of BART plays important roles in maintaining Rac1 in a constitutively inactive state and in the suppression of the malignant phenotype.

Dynamic actin remodeling processes at the leading edge of migrating cells are complex and involve increased actin filament severing, capping, and dendritic branching [39]. Rho GTPases and their effectors are key intracellular signaling molecules that coordinate cytoskeletal remodeling that is required for cell spreading, motility, and cell shape changes [40]. The results of our immunofluorescence studies show that knockdown of BART induces peripheral rearrangements of the actin cytoskeleton in S2-013 cells cultured on fibronectin (Figure 6, *A* and *B*), and that exogenously overexpressed BART significantly inhibited peripheral actin-cytoskeletal rearrangements in BART RNAi cells (Figure 6*D*). Dynamic, actin-based plasma membrane protrusions that control growth cone path finding include lamellipodia, in which the actin cytoskeleton assumes a crosslinked and branched meshwork, and filopodia, which consist of parallel bundles of actin filaments protruding from the growth cone or lamellipodial margin [41]. Our results indicate that BART is a physiological inhibitor that elicits actin redistribution, leading to peripheral actin rearrangements. Interestingly, peripheral actin rearrangements were not induced when BART RNAi S2-013 cells plated on fibronectin were treated with the Rac1 inhibitor (Figure 6*C*). Given that BART regulates the level of Rac1 activity as well as peripheral actin rearrangements, BART must be associated with the regulation of membrane ruffles, resulting in the inhibition of PDAC cell motility and invasion.

The findings presented in this study are supportive of the pivotal roles of BART in the coordinated regulation of cortical actin changes through the regulation of the level of Rac1 activity. We have established the functional significance of the interaction of BART with active forms of Rac1, which mediates the anti-invasive effect of BART in PDAC cells.

Acknowledgments

The authors thank Michael Hollingsworth for many helpful experimental suggestions. The authors also thank Keith Johnson for kindly providing us with the pGEX-PAK-CRIB and pGEX-Rhotekin plasmids and Aki Tanouchi for her excellent technical assistance.

References

[1] Sharer JD and Kahn RA (1999). The ARF-like 2 (ARL2)–binding protein, BART. Purification, cloning, and initial characterization. *J Biol Chem* **274**(39), 27553–27561.

[2] Clark J, Moore L, Krasinskas A, Way J, Battey J, Tamkun J, and Kahn RA (1993). Selective amplification of additional members of the ADP-ribosylation factor (ARF) family: cloning of additional human and *Drosophila* ARF-like genes. *Proc Natl Acad Sci USA* **90**(19), 8952–8956.

[3] Zhou C, Cunningham L, Marcus AI, Li Y, and Kahn RA (2006). Arl2 and Arl3 regulate different microtubule-dependent processes. *Mol Biol Cell* **17**(5), 2476–2487.

[4] Taniuchi K, Nishimori I, and Hollingsworth MA (2011). Intracellular CD24 inhibits cell invasion by post-transcriptional regulation of BART through interaction with G3BP. *Cancer Res* **71**(3), 895–905.

[5] Taniuchi K, Iwasaki S, and Saibara T (2011). BART inhibits pancreatic cancer cell invasion by inhibiting the function of ARL2 in RhoA inactivation. *Int J Oncol* **39**(5), 1243–1252.

[6] Etienne-Manneville S and Hall A (2002). Rho GTPases in cell biology. *Nature* **420**(6916), 629–635.

[7] Mackay DJ and Hall A (1998). Rho GTPases. *J Biol Chem* **273**(33), 20685–20688.

[8] Hall A (1998). Rho GTPases and the actin cytoskeleton. *Science* **279**(5350), 509–514.

[9] Slater SJ, Seiz JL, Stagliano BA, and Stubbs CD (2001). Interaction of protein kinase C isozymes with Rho GTPases. *Biochemistry* **40**(14), 4437–4445.

[10] Eiseler T, Döppler H, Yan IK, Kitatani K, Mizuno K, and Storz P (2009). Protein kinase D1 regulates cofilin-mediated F-actin reorganization and cell motility through slingshot. *Nat Cell Biol* **11**(5), 545–556.

[11] Muromoto R, Sekine Y, Imoto S, Ikeda O, Okayama T, Sato N, and Matsuda T (2008). BART is essential for nuclear retention of STAT3. *Int Immunol* **20**, 395–403.

[12] Aznar S, Valerón PF, del Rincon SV, Pérez LF, Perona R, and Lacal JC (2001). Simultaneous tyrosine and serine phosphorylation of STAT3 transcription factor is involved in Rho A GTPase oncogenic transformation. *Mol Biol Cell* **12**(10), 3282–3294.

[13] Debidda M, Wang L, Zang H, Poli V, and Zheng Y (2005). A role of STAT3 in Rho GTPase-regulated cell migration and proliferation. *J Biol Chem* **280**(17), 17275–17285.

[14] Iwamura T, Katsuki T, and Ide K (1987). Establishment and characterization of a human pancreatic cancer cell line (SUIT-2) producing carcinoembryonic antigen and carbohydrate antigen 19-9. *Jpn J Cancer Res* **78**(1), 54–62.

[15] Gao Y, Dickerson JB, Guo F, Zheng J, and Zheng Y (2004). Rational design and characterization of a Rac GTPase-specific small molecule inhibitor. *Proc Natl Acad Sci USA* **101**(20), 7618–7623.

[16] Huttenlocher A, Lakonishok M, Kinder M, Wu S, Truong T, Knudsen KA, and Horwitz AF (1998). Integrin and cadherin synergy regulates contact inhibition of migration and motile activity. *J Cell Biol* **141**(2), 515–526.

[17] Waterman-Storer CM, Salmon WC, and Salmon ED (2000). Feedback interactions between cell-cell adherens junctions and cytoskeletal dynamics in newt lung epithelial cells. *Mol Biol Cell* **11**(7), 2471–2483.

[18] Betson M, Lozano E, Zhang J, and Braga VM (2002). Rac activation upon cell-cell contact formation is dependent on signaling from the epidermal growth factor receptor. *J Biol Chem* **277**(40), 36962–36969.

[19] Braga VM, Betson M, Li X, and Lamarche-Vane N (2000). Activation of the small GTPase Rac is sufficient to disrupt cadherin-dependent cell-cell adhesion in normal human keratinocytes. *Mol Biol Cell* **11**(11), 3703–3721.

[20] Kovacs EM, Ali RG, McCormack AJ, and Yap AS (2002). E-cadherin homophilic ligation directly signals through Rac and phosphatidylinositol 3-kinase to regulate adhesive contacts. *J Biol Chem* **277**(8), 6708–6718.

[21] Schaefer A, Miertzschke M, Berken A, and Wittinghofer A (2011). Dimeric plant RhoGAPs are regulated by its CRIB effector motif to stimulate a sequential GTP hydrolysis. *J Mol Biol* **411**(4), 808–822.

[22] Ridley AJ and Hall A (1992). The small GTP-binding protein rho regulates the assembly of focal adhesions and actin stress fibers in response to growth factors. *Cell* **70**(3), 389–399.

[23] Schwartz MA, Schaller MD, and Ginsberg MH (1995). Integrins: emerging paradigms of signal transduction. *Annu Rev Cell Dev Biol* **11**(1), 549–599.

[24] Kimura K, Kawamoto K, Teranishi S, and Nishida T (2006). Role of Rac1 in fibronectin-induced adhesion and motility of human corneal epithelial cells. *Invest Ophthalmol Vis Sci* **47**(10), 4323–4329.

[25] Nobes CD and Hall A (1995). Rho, Rac, and Cdc42 GTPases regulate the assembly of multimolecular focal complexes associated with actin stress fibers, lamellipodia, and filopodia. *Cell* **81**(1), 53–62.

[26] Price LS, Leng J, Schwartz MA, and Bokoch GM (1998). Activation of Rac and Cdc42 by integrins mediates cell spreading. *Mol Biol Cell* **9**(7), 1863–1871.

[27] Di Ciano C, Nie Z, Szászi K, Lewis A, Uruno T, Zhan X, Rotstein OD, Mak A, and Kapus A (2002). Osmotic stress–induced remodeling of the cortical cytoskeleton. *Am J Physiol Cell Physiol* **283**(3), C850–C865.

[28] Lewis A, Di Ciano C, Rotstein OD, and Kapus A (2002). Osmotic stress activates Rac and Cdc42 in neutrophils: role in hypertonicity-induced actin polymerization. *Am J Physiol Cell Physiol* **282**(2), C271–C279.

[29] Baumgart M, Heinmöller E, Horstmann O, Becker H, and Ghadimi BM (2005). The genetic basis of sporadic pancreatic cancer. *Cell Oncol* **27**(1), 3–13.

[30] Ahrendt SA and Pitt HA (2002). Surgical management of pancreatic cancer. *Oncology* **16**(6), 725–734.

[31] Sceffzek K, Ahmadian MR, and Wittinghofer A (1998). GTPase-activating proteins: helping hands to complement an active site. *Trends Biochem* **23**(7), 257–262.

[32] Bhamidipati A, Lewis SA, and Cowan NJ (2000). ADP ribosylation factor-like protein 2 (Arl2) regulates the interaction of tubulin-folding cofactor D with native tubulin. *J Cell Biol* **149**(5), 1087–1096.

[33] Liliental J, Moon SY, Lesche R, Mamillapalli R, Li D, Zheng Y, Sun H, and Wu H (2000). Genetic deletion of the Pten tumor suppressor gene promotes cell motility by activation of Rac1 and Cdc42 GTPases. *Curr Biol* **10**(7), 401–404.

[34] Guo F, Gao Y, Wang L, and Zheng Y (2003). $p19^{Arf}$-p53 tumor suppressor pathway regulates cell motility by suppression of phosphoinositide 3-kinase and Rac1 GTPase activities. *J Biol Chem* **278**(16), 14414–14419.

[35] Guo F and Zheng Y (2004). Involvement of Rho family GTPases in $p19^{Arf}$- and p53-mediated proliferation of primary mouse embryonic fibroblasts. *Mol Cell Biol* **24**(3), 1426–1438.

[36] Jin K, Park S, Ewton DZ, and Friedman E (2007). The survival kinase Mirk/Dyrk1B is a downstream effector of oncogenic K-*ras* in pancreatic cancer. *Cancer Res* **67**(15), 7247–7255.

[37] Takai Y, Sasaki T, and Matozaki T (2001). Small GTP-binding proteins. *Physiol Rev* **81**(1), 153–208.

[38] Van Aelst L and D'Souza-Schorey C (1997). Rho GTPases and signaling networks. *Genes Dev* **11**(18), 2295–2322.

[39] Bamburg JR, McGough A, and Ono S (1999). Putting a new twist on actin: ADF/cofilins modulate actin dynamics. *Trends Cell Biol* **9**(9), 364–370.

[40] Ridley AJ (2001). Rho GTPases and cell migration. *J Cell Sci* **114**(15), 2713–2722.

[41] Gallo G and Letourneau PC (2004). Regulation of growth cone actin filaments by guidance cues. *J Neurobiol* **58**(1), 92–102.

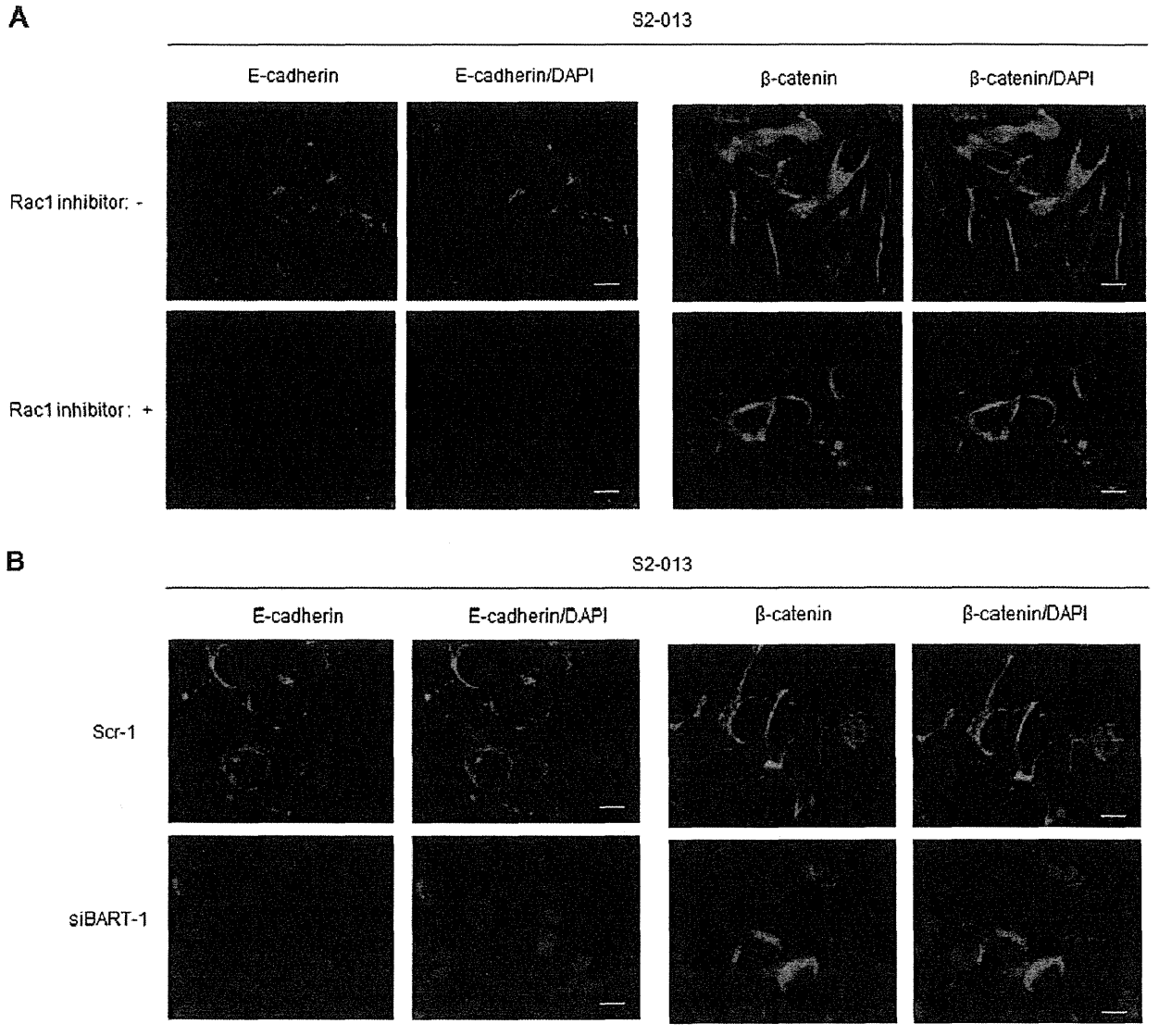

Figure W1. BART functions in regulation of the stability of cell-cell contacts in a Rac1-independent manner. (A) S2-013 cells were pre-treated with or without the Rac1 inhibitor (NSC23766), and immunocytochemical staining was performed using anti–E-cadherin and anti–β-catenin antibodies (green). Blue indicates DAPI staining. Bars, 10 μm. (B) Representative E-cadherin and β-catenin staining (green) in scrambled control (Scr-1) and BART RNAi (siBART-1) S2-013 cells. Blue indicates DAPI staining. Bars, 10 μm.

Original Communication

Abnormality in Expression Levels of Gluconeogenesis-Related Genes by High-Dose Supplementation with Pyridoxamine in Mice

Huong Thi Viet Do[1], Katsumi Toda[2], Toshiji Saibara[3], and Toshiharu Yagi[1]

[1]Faculty of Agriculture and Agricultural Science Program, Graduate School of Integral Arts and Science, Kochi University, Nankoku, Kochi, Japan
[2]Department of Biochemistry, Kochi University, School of Medicine, Nankoku, Kochi, Japan
[3]Department of Gastroenterology and Hepatology, Kochi University, School of Medicine, Nankoku, Kochi, Japan

Received: April 27, 2011; Accepted: November 4, 2011

Abstract: Pyridoxamine supplementation caused the alteration of the expression of genes encoding six gluconeogenesis-related proteins. The expression levels of phosphoenolpyruvate carboxykinase, pyruvate kinase, and pyruvate dehydrogenase kinase 4 in the pyridoxamine-supplemented mice were higher than those in the control mice. In contrast, the pyridoxamine supplementation caused lower expression levels of peroxisome proliferator-activated receptor-γ coactivator-1α, carbohydrate response element-binding protein, glucocorticoid receptor, and glucose-6-phosphatase. The pyridoxamine-supplemented mice showed significantly low glucose clearance in a glucose tolerance test, but they showed no symptoms of diabetes, which was estimated according to the levels of hemoglobin A1c and blood glucose. Pyruvate challenge testing suggested that pyridoxamine supplementation enhanced gluconeogenic activity from pyruvate. The results showed that a high-dose of pyridoxamine may require a careful inquiry concerning its validity.

Key words: pyridoxamine, gene expression, gluconeogenesis, phosphoenolpyruvate carboxykinase, diabetes, diabetic complications.

Introduction

Pyridoxamine is one of the family of vitamin B_6 compounds, which consists of six compounds; i.e. pyridoxal, pyridoxamine, pyridoxine, pyridoxal 5′-phosphate, pyridoxamine 5′-phosphate, and pyridoxine 5′-phosphate. Pyridoxal 5′-phosphate is the coenzyme form for many enzymes involved in amino acid and carbohydrate metabolism, and plays a key role in the nutritional function of vitamin B_6. The other forms show the same nutritional efficiency because they are converted into pyridoxal 5′-phosphate [1]. Pyridoxamine inhibits

DOI 10.1024/0300–9831/XXXX

specifically the formation of advanced glycation end products (AGEs) and toxic effects of reactive oxygen species, and scavenges reactive carbonyl compounds [2]. Thus, its pharmacological potential for treatment of diabetic nephropathy [3], diabetic retinopathy [4], and hyperlipidemia [5] has been demonstrated.

Vitamin B_6 supplementation has been shown to be beneficial in treating several disorders like atherosclerosis [6] and gyrate atrophy [7]. The risk of toxicity of vitamin B_6 supplementation has generally been thought to be low. However, it was found that pyridoxine hydrochloride caused neuropathy at intakes of 200 mg per day or more, which is about 140-fold higher than the daily intake from foods, when it was used to alleviate symptoms of carpal tunnel syndrome [8]. In some cases, intakes of 100–300 mg per day caused neurotoxicity. An *in vitro* study with a model system of dorsal root ganglion neurons in culture showed that very high doses of pyridoxamine, pyridoxine, and pyridoxal are neurotoxic in humans and other animals [9]. Ataxia developed in rats fed diets containing 5.9 mg of pyridoxine/g by the 15th week [10]. Pyridoxine caused neuropathy in a human at intakes of 1000 mg per day or more, which is about 800 times the daily intake from foods [11]. The toxicity studies on animals and humans have usually been performed using pyridoxine hydrochloride as a source of vitamin B_6. Little is known about the mechanism of vitamin B_6 toxicity. Because pyridoxine is converted into pyridoxal 5′-phosphate, which modulates the expression of a variety of genes that respond to hormones [12], a high concentration of pyridoxine may change the expression levels of many genes. Pyridoxamine is also converted into pyridoxal 5′-phosphate, and may change the expression level of genes. As far as we know, no study has reported about the effect of pyridoxamine on the expression level of genes. Because pyridoxamine is better than aminoguanidine as an AGE inhibitor in terms of safety [13], and can be used in large amounts to alleviate symptoms of diabetic complications as described above, its effect on gene expression should be elucidated.

Here, for the first time, we have studied the effect of pyridoxamine supplementation on the expression levels of gluconeogenesis-related genes in mice, and found that it changed their expression levels, and decreased the glucose clearance in the blood of the animals without an incidence of the symptoms of diabetes.

Materials and methods

Animals

Experimental procedures involving mice were approved by the Institutional Animal Care and Use Committee. Male mice of the C57BL/6 genetic background were housed in specific pathogen-free conditions in the animal facility at Kochi University. The mice were kept in the same room at 22–25 °C with a regular 12-hour light/dark cycle and fed with a standard rodent chow (NMF; Oriental Yeast, Tokyo, Japan) and water *ad libitum*.

Reagents and treatments

Pyridoxamine dihydrochloride (4-aminomethyl-3-hydroxy-2-methyl-5-hydroxymethylpyridine dihydrochloride) was purchased from Tokyo Chemical Company, Ltd. (Tokyo, Japan). Ten and six male mice, respectively, were given drinking water with and without pyridoxamine dihydrochloride (1 g/L) for 3 months, starting at 2 months of age. The mice consumed 3–5 mg of pyridoxamine dihydrochloride per day. The value is equivalent to 4.5–7.5 g of pyridoxamine in humans weighing 60 kg.

Biochemical characterization

The hemoglobin A1c (HbA1c) levels were measured at age of 5 months by immunoassay (DCA 2000 system, Bayer Diagnostics, Elkhart, IN). Glucose levels in blood were measured using Glutest Ace and Glutest Sensor (Sanwa Kagaku Kenkyusho Co., Nagoya, Japan).

Glucose tolerance, insulin tolerance and pyruvate challenge tests

90,

Mice were fasted for 16 hours overnight with full access to water. The glucose tolerance test (GTT) was done with the mice as described previously [14]. In brief, glucose dissolved in a physiological saline solution was injected intraperitoneally (1 mg/g of body

15,

t). Glucose levels in tail bloods, collected by vein nicks at 0, 30, 60, and 120 minutes after the injection, were measured. Insulin sensitivity was assessed using an insulin tolerance test (ITT) as described previously [14]. For the pyruvate challenge test, the mice were injected intraperitoneally with pyruvate (2 mg/g of

15,

90,

body weight) dissolved in saline, and then glucose concentrations in tail bloods were collected by vein nicks at 0, 30, 60, and 120 minutes after the injection were measured [15]. The mice were injected intraperitoneally with human recombinant insulin (Novo Nordisk Pharma Ltd) at a dose of 0.75 mU/g of body weight, and then glucose concentrations in tail bloods were measured at 0, 10, 30, 60 and 120 minutes.

Statistical analysis

All data are presented as mean ± SD. The statistical significance was examined by the independent-measures *t*-test. The Excel software was used. P values less than 0.05 were considered as statistically significant.

Quantitative real-time PCR (qRT-PCR) with SYBR green

Total RNA was prepared from the livers by the method of Zarlenga and Gamble [16]. The total RNA (1 µg) was reverse-transcribed using the M-MLV Superscript™ II Reverse Transcriptase (Life Technologies Japan Ltd. Tokyo, Japan) for first-strand cDNA synthesis with 0.8 µM oligo (dT) primer (Life Technologies Japan, Tokyo, Japan) according to the manufacturer's instructions. In brief, the RNA and the primer were mixed, and then the mixture was incubated at 65 °C for 10 minutes, followed by cooling on ice for 5 minutes. The first-strand cDNA synthesis was started by addition of a transcription mixture to the cooled mixture, and then the mixture was incubated at 37 °C for 1 hour for the reverse transcription reaction. All of the reaction

Table I: Primers for quantitative real-time PCR.

Proteins (ID/Version)	Primers
Carbohydrate response element-binding protein (ChREBP NM_021455.3)	
forward	CTGGGGACCTAAACAGGAGC
reverse	GAAGCCACCCTATAGCTCCC
Cyclophilin A (NM_008907.1)	
forward	ATGGCACTGGCGGCAGGTCC
reverse	TTGCCATTCCTGGACCCAAA
Glucocorticoid receptor (NM_008173.3)	
forward	AAAGAGCTAGGAAAAGCCATTGTC
reverse	TCAGCTAACATCTCTGGGAATTCA
Glucose 6-phosphatase (~~G-6-Pase~~ NM_008061.3)	
forward	TGAAACTTTCAGCCACATCCG
reverse	GCAGGTAGAATCCAAGCGCGAA
Peroxisome proliferator-activated receptor γ coactivator 1-α (Pgc-1α NM_008904)	
forward	CCCTGCCATTGTTAAGACC
reverse	TGCTGCTGTTCCTGTTTTC
Phosphoenolpyruvate carboxykinase (PEPCK NM_011044.2)	
forward	CACCAACGTGGCTGAGACTA
reverse	CTACGGCCACCAAAGATGAT
Pyruvate dehydrogenase kinase 4 (~~PDK4~~ NM_013743.2)	
forward	TTTCTCGTCTCTACGCCAAG
reverse	GATACACCAGTCATCAGCTTCG
Pyruvate kinase (~~PK~~ NM_013631.2)	
forward	TACCACCGCCAG TTG TTTG
reverse	GCGGCCAGTCTTTGTCAGC

Glc-6-Pase

α

Pdk4

Pklr

mixture containing the synthesized cDNA was diluted 1:5 with H_2O and stored at –20 °C.

Quantitative PCR (qRT-PCR) was done with a Thermal Cycler Dice® real time system (TaKaRa Bio Inc., Shiga, Japan) using SYBR®Premix ExTaq ™II mix (TaKaRa Bio Inc., Shiga, Japan). The PCR reaction mixture (20 µL) contained 2 µL cDNA (8 ~~em~~/µL), 1 µL (10 µM) of each primer shown in Table I, 10 µL Premix ExTaq ™II mix, and H_2O. After initial denaturation (one cycle at 95 °C for 30 seconds), 40 cycles of amplification (95 °C for 5 seconds, 60 °C for 20 seconds) were performed. The production of a single amplified product was confirmed by a dissociation protocol according to the manufacturer's instruction and an electrophoretic analysis on 10 % polyacrylamide gels [17]. Relative gene expression levels were calculated with the comparative CT method using cyclophilin A (peptidyl-prolyl cis-trans isomerase A) as an internal reference gene. The expression levels in the control mice were set as 1. Differences between the control and the pyridoxamine-supplemented mice were presented as fold-differences.

Results

Biochemical parameters

The levels of HbA1c and body weight at age of 5 months in the control group were 4.2 ± 0.4 % and 34.4 ± 1.8 g, respectively. Those in the pyridoxamine-supplemented group were 4.1 ± 0.2 % and 33.8 ± 1.0 g, respectively. There were no significant differences between these values. The mean levels of fasting blood glucose at the age of 5 months in the control (88.9 ± 8.6 mg/dL) and pyridoxamine-supplemented groups (99.3 ± 5.7 mg/dL) were not significantly different either. The results showed that the prolonged supplementation with pyridoxamine caused no symptom of diabetes.

ng

Expression of mRNA for enzymes involved in gluconeogenesis

30

Liver mRNA levels of six gluconeogenesis-related proteins in the control and pyridoxamine-supplemented mice were compared as shown

Pklr

The mRNA level for phosphoenolpyruvate carboxykinase (PEPCK), which plays an important role in gluconeogenesis from non-sugar carbon [18], was 1.38-fold higher than the control mice. The expression level for pyruvate kinase (~~PK~~), which is involved in glycolysis, converts phosphoenolpyruvate into pyruvate, and thus inhibits gluconeogenesis, was also 1.22-fold higher in the liver of the pyridoxamine-supplemented mice. The expression levels of Pgc-1α and glucocorticoid receptor (GR) in the pyridoxamine-supplemented mice were 0.66- and 0.75-fold lower than that of the control mice, respectively. Pgc-1α is a member of the PPARγ coactivator-1 (Pgc-1) family and plays a central role in a regulatory network governing mitochondrial biogenesis [19]. The lower expression level of Pgc-1α suggested that mitochondrial biogenesis and/or energy production modestly declined in the liver via pyridoxamine supplementation. The complex of Pgc-1α, GR, and hepatocyte nuclear factor 4α (HNF4α) has been shown to be involved in augmentation of the expression level of PEPCK [20]. The results suggested that pyridoxamine changed the metabolism of glucose in mice, although it caused no incidence of diabetes.

Table II: Expression of mRNA for gluconeogenesis-related proteins.

Proteins	Fold differences[a]
Phosphoenolpyruvate carboxykinase	1.38 ± 0.11[b]
Pyruvate kinase	1.22 ± 0.11[b]
Pyruvate dehydrogenase kinase 4	1.10 ± 0.20
Glucose 6-phosphatase	0.88 ± 0.11
Glucocorticoid receptor	0.75 ± 0.05[b]
Carbohydrate response element-binding protein	0.74 ± 0.02[b]
Peroxisome proliferator-activated receptor γ coactivator 1-α	0.66 ± 0.09[b]

[a]Fold differences in expression levels of mRNA between the control (1.00) and the pyridoxamine-supplemented mice.
[b]Significantly different from the control.

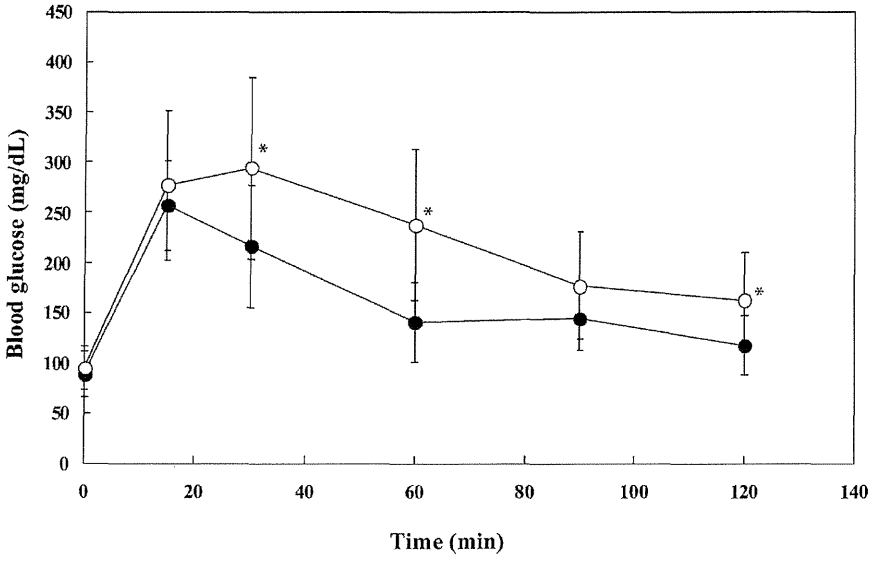

Figure 1: Glucose tolerance test. Blood glucose concentrations in the control (closed circles) and pyridoxamine-supplemented (open circles) mice were determined, after the glucose injection.
*$p < 0.05$ versus the corresponding value for the control mice.

Glucose tolerance, insulin tolerance, and pyruvate challenge tests

The effect of pyridoxamine-supplementation on glucose intolerance was examined. The pyridoxamine-supplemented mice showed a symptom of glucose intolerance, with a significantly higher glucose level from 30 minutes to 120 minutes after the glucose injection (Figure 1). In contrast, the pyridoxamine-supplemented mice did not show differences in insulin sensitivity, and thus had the same pattern of time-dependent changes in the blood glucose level as shown in Figure 2. Interestingly, administration of pyruvate, a substrate for gluconeogenesis, resulted in a significant increase in blood glucose concentration at 120 minutes in the pyridoxamine-supplemented mice (Figure 3). The results clearly showed that pyridoxamine supplementation deteriorated glucose clearance in blood.

Discussion

As pyridoxamine is implicated to have the pharmacological potential for treatment of complications

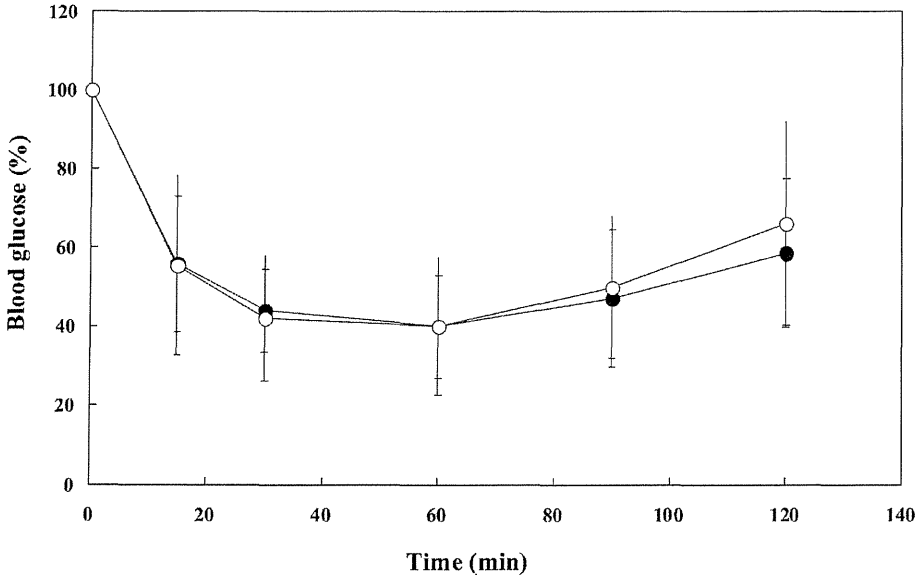

Figure 2: Insulin tolerance test. The changes in blood glucose concentrations in the control (closed circles) and pyridoxamine-supplemented (open circles) mice were determined after the insulin injection. The glucose concentration in the mice just before the injection was 100 %.

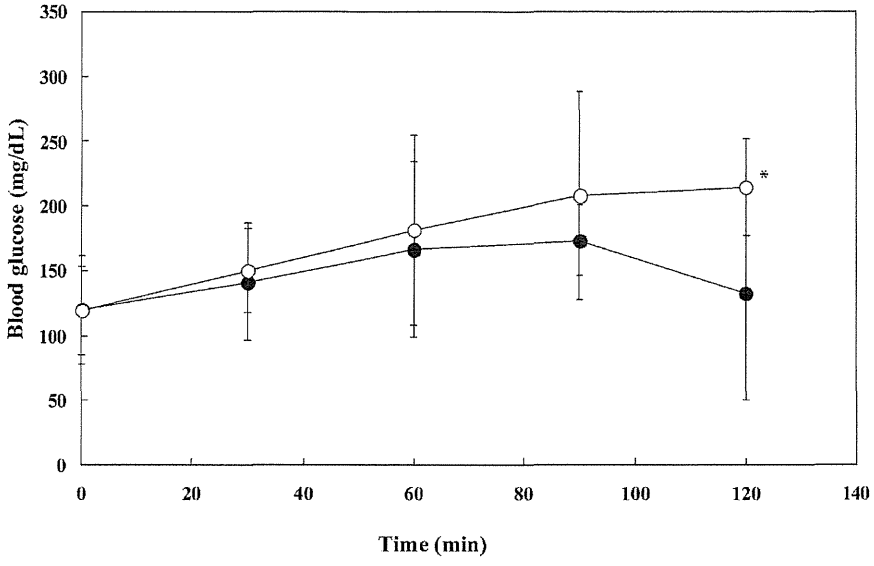

Figure 3: Pyruvate challenge test. Blood glucose concentrations in the control (closed circles) and pyridoxamine-supplemented (open circles) mice were determined after the pyruvate injection. *p<0.05 versus the corresponding value for the control mice.

associated with diabetic mellitus [2–5], effects of its long-term high-dose administration were evaluated on hepatic gene expression levels as well as on serum glucose levels. The analysis revealed marginal effects on the genes related to glucose metabolism; 1.2–1.3 fold enhancement in the mRNA levels for PEPCK and PK, whereas decreases by 25~35 % for ~~Chrebp~~, Pgc-1α, and GR over the control levels, respectively. Physiological relevance of these subtle effects on the mRNA levels remains to be elucidated, although the differences are statistically significant. Apparently additional studies are required to elucidate the mechanism of modulation of gene expression by pyridoxamine. However, pyridoxal 5′-phosphate produced from pyridoxamine [1] in the liver may play a key role because it acts as a modulator of both steroid hormone receptor-mediated gene expression and albumin gene expression [21]. Thus, it would be valuable to examine whether pyridoxine-supplementation also modulates the gluconeogenesis-related genes examined here.

The supplementation with pyridoxamine did not cause symptoms (based on the levels of blood glucose and HbA1c) of diabetes in the mice in accordance with the results reported previously [22]. The results of the insulin tolerance test also supported this phenomenon. However, it was found that the pyridoxamine-supplemented mice showed a slower clearance of glucose in blood after glucose injection than the control mice. Based on the results of glucose tolerance test (GTT) and insulin tolerance test (ITT) analysis, we speculate that pyridoxamine might cause impairment in pancreatic function, including synthesis/secretion of insulin or sensory activity to serum glucose levels. Furthermore, pyridoxamine-supplemented mice showed higher blood glucose levels at 120 minutes after the injection of pyruvate, suggesting that gluconeogenic activity from pyruvate was enhanced. Because pyridoxal 5′-phosphate shows considerable inhibition of cathepsins at high concentrations [23], it is plausible that gluconeogenic activity using pyruvate as a substrate might be enhanced to meet systemic demands for glucose in the pyridoxamine-supplemented mice. Taken together, our present study thus indicates that supplementation with pyridoxamine for the long term may decrease whole-body glucose disposal and/or glucose uptake function in tissue sites such as muscle and adipose.

The results showed that the pyridoxamine-supplementation changed the expression pattern of gluconeogenesis-related genes examined. The nutrigenomic approach will indicate the alteration of gene expression patterns of many other functional genes. In this study, the dose of pyridoxamine was very high (the equivalent of 4.5–7.5 g for humans weighing 60 kg). Because, the toxicity of high-dose pyridoxine-supplementation is well known [11], supplementation of such a high amount of pyridoxamine to humans is beyond the realm of possibility. However, a high dose of pyridoxamine over a long period of time to alleviate symptoms of diabetic complications may require a careful inquiry concerning its validity, although pyridoxamine-supplementation is beneficial for treatment of complications associated with diabetic mellitus [2–5].

References

1. Spinneker, A., Sola, R., Lemmen, V., Castillo, M.J., Pietrzik, K. and González-Gross, M. (2007) Vitamin B_6 status, deficiency and its consequences – An overview. Nutr. Hosp. 22, 7.

2. Voziyan, P.A. and Hudson, B.G. (2005) Pyridoxamine. The many virtues of a Maillard reaction inhibitor. Ann. N. Y. Acad. Sci. 1043, 807.

3. Waanders, F., Van Den Berg, E., Nagai, R., Van Veen, I., Navis, G. and Van Goor, H. (2008) Renoprotective effects of the AGE-inhibitor pyridoxamine in experimental chronic allograft nephropathy in rats. Nephro. Dial. Transplant. 23, 518.

4. El-Hossary, G.G., El-Shazly, A.H.M., Ahmed, N.S., Mansour, S.M. and Mohamed, A.S. (2010) Effect of pyridoxamine on diabetic retinopathy and diabetes-induced deterioration of serum lipids and creatinine in experimental animals. J. Appl. Sci. Res. 6, 1316.

5. Metz, T.O., Alderson, N.L., Thorpe, S.R. and Baynes, J.W. (2003) Pyridoxamine, an inhibitor of advanced glycation and lipoxidation reactions: A novel therapy for treatment of diabetic complications. Arch. Biochem. Biophys. 419, 41.

6. Ellis, J.M. and McCully, K.S. (1995) Prevention of myocardial infarction by vitamin B6. Res. Commun. Mol. Pathol. Pharmacol. 89, 208.

7. Tanzer, F., Firat, M., Alagoz, M. and Erdogan, H. (2011) Gyrate atrophy of the choroid and retina with hyperornithinemia, cystinuria and lysinuria responsive to vitamin B6. BMJ Case Reports. In press.

8. Driskell, J.A. (1994) Vitamin B-6 requirements of humans. Nutr. Res. 14, 293.

9. Windebank, A.J. (1985) Neurotoxicity of pyridoxine analogs is related to coenzyme structure. Neurochem. Pathol. 3, 159.

10. Bacon, L.M. and Turk, D.E. (1987) Chronic pyridoxine intoxication in rats. Nutr. Rep. Int. 35, 1035.

11. Katan, M.B. (2005) How much vitamin B_6 is toxic? Ned. Tijdschr. Geneeskd. 149, 2545.

12. Oka, T., Komori, N., Kuwahata, M., Okada, M. and Natori, Y. (1995) Vitamin B_6 modulates expression of albumin gene by inactivating tissue-specific DNA-binding protein in rat liver. Biochem. J. 309, 243.

13. Turgut, F. and Bolton, W.K. (2010) Potential New Therapeutic Agents for Diabetic Kidney Disease. Amer. J. Kidney Diseases 55 (5), 928–940.

14. Toda, K., Hayashi, Y. and Saibara, T. (2010) Deletion of tumor necrosis factor-α receptor type 1 exacerbates insulin resistance and hepatic steatosis in aromatase knockout mice. Biochim. Biophys. Acta 1801, 655.

15. Miyake, K., Ogawa, W., Matsumoto, M., Nakamura, T., Sakaue, H. and Kasuga, M. (2002) Hyperinsulinemia, glucose intolerance, and dyslipidemia induced by acute inhibition of phosphoinositide 3-kinase signaling in the liver. J. Clin. Invest. 110, 1483.

16. Zarlenga, D.S. and Gamble, H.R. (1987) Simultaneous isolation of preparative amounts of RNA and DNA from Trichinella spiralis by cesium trifluoroacetate isopycnic centrifugation. Anal. Biochem. 162, 569.

17. Sambrook, J. and Russell, D.W. (2001) Protocol 9, Neutral polyacrylamide gel electrophoresis. In: Molecular Cloning, A laboratory manual. 3rd edition, pp. 5.40–5.46, Cold Spring Harbor Laboratory Press, New York.

18. Tilghman, S.M., Hanson, R.W. and Ballard, F.J. (1976) Gluconeogenesis: Its Regulation in Mammalian Species (Hanson, R. W. & Mehlman, M. A., eds.) pp. 47–91, Wiley-Interscience, New York.

19. Scarpulla, R.C. (2011) Metabolic control of mitochondrial biogenesis through the PGC-1 family regulatory network. Biochim. Biophys. Acta 1813, 1269.

20. Hanson, R.W. and Reshef, L. (1997) Regulation of phosphoenolpyruvate carboxykinase (GTP) gene expression. Annu. Rev. Biochem. 66, 581.

21. Oka, T. (2001) Modulation of gene expression by vitamin B_6. Nutr. Res. 14, 257.

22. Degenhardt, T.P., Alderson, N.L., Arrington, D.D., Beattie, R.J,. Basgen, J.M., Steffes, M.W., Thorpe, S.R. and Baynes, J.W. (2002) Pyridoxamine inhibits early renal disease and dyslipidemia in the streptozotocin-diabetic rat. Kidney Int. 61, 939.

23. Katunuma, N., Matsui, A., Inubushi, T., Murata, E., Kakegawa, H., Ohba, Y., Turk, D., Turk, V., Tada, Y. and Asao, T. (2000) Structure-based development of pyridoxal propionate derivatives as specific inhibitors of cathepsin K *in vitro* and *in vivo*. Biochem. Biophys. Res. Commun. 267, 850.

Toshiharu Yagi

Faculty of Agriculture and Agricultural Science Program
Graduate School of Integral Arts and Science
Kochi University, Nankoku
Kochi 783–8502
Japan
Tel. & Fax: +81–88–864–5191
yagito@kochi-u.ac.jp

Molecular and Cellular Endocrinology 362 (2012) 176–182

Contents lists available at SciVerse ScienceDirect

Molecular and Cellular Endocrinology

journal homepage: www.elsevier.com/locate/mce

17β-Estradiol is critical for the preovulatory induction of prostaglandin E_2 synthesis in mice

Katsumi Toda [a,*], Masafumi Ono [b], Koh-ichi Yuhki [c], Fumitaka Ushikubi [c], Toshiji Saibara [b]

[a] Department of Biochemistry, Kochi University, School of Medicine, Nankoku, Kochi 783-8505, Japan
[b] Department of Gastroenterology and Hepatology, Kochi University, School of Medicine, Nankoku, Kochi 783-8505, Japan
[c] Department of Pharmacology, Asahikawa Medical University, Asahikawa, Hokkaido 078-8510, Japan

ARTICLE INFO

Article history:
Received 28 February 2012
Received in revised form 8 June 2012
Accepted 12 June 2012
Available online 17 June 2012

Keywords:
Aromatase-knockout mouse
Cyclooxygenase 2
Estrogen
Prostaglandin E_2
Ovulation

ABSTRACT

Aromatase-deficient (ArKO) mice are totally anovulatory due to insufficient estrogen production. However, sequential administrations of high doses of 17β-estradiol (E2) and gonadotropins were found to induce ovulation in these mice. Here, we examined how the ovulatory stimulation for ArKO mice alters the expressions of genes related to prostaglandin (PG) E_2 metabolism and ovarian contents of PGE_2, as PGE_2 is one of the critical mediators of ovulatory induction. The ovulatory stimulation significantly increased mRNA expressions of prostaglandin-endoperoxide synthase 2, PGE_2 receptor type 4 and sulfotransferase family 1E, member 1, in preovulatory ArKO ovaries. In contrast, it suppressed the mRNA expression of 15-hydroxyprostaglandin dehydrogenase. Furthermore, significant elevation in the PGE_2 contents was detected in the preovulatory ovaries of ArKO mice after stimulation with E2 plus ovulatory doses of gonadotropins. Thus, these analyses demonstrate a requirement of E2 for the preovulatory enhancement of PGE_2 synthesis, leading to future success in ovulation.

1. Introduction

The aromatase gene (*Cyp19a*), belonging to the cytochrome P450 superfamily, encodes an enzyme that catalyzes the conversion of androgens to estrogens (Simpson et al., 1994). Estrogen plays pivotal roles in the control of the cyclic pattern of ovarian follicular development (Drummond and Findlay, 1999). The lack of estrogenic actions, probably through ERβ, was suggested to be related to the follicular atresia, leading to the early exhaustion of follicles (Carson et al., 1981; Cheng et al., 2002). Although the exact roles of E2 in the ovary have not been fully defined, E2, in conjunction with FSH and LH, increases the number of cAMP binding sites (Richards and Rolfes, 1980), stimulates the proliferation and facilitates the differentiating actions of FSH and LH in granulosa cells (Bley et al., 1997; Robker and Richards, 1998). E2 was also demonstrated to stimulate the extent of gap junctions among granulosa cells (Merk et al., 1972). Aromatase gene-knockout (ArKO) mouse has been proved to be a useful animal model to study the physiological roles of estrogens (Fisher et al., 1998; Toda et al., 2001; Britt et al., 2004). ArKO females are completely refractory to all kinds of ovulatory stimuli, even with administration of conventional ovulatory doses of gonadotropins (Fisher et al., 1998; Toda et al., 2001; Britt et al., 2004). However, the mechanisms involved in this unresponsiveness have not been elucidated.

Ovulation is a dynamic reproductive phenomenon regulated strictly by pituitary hormones, follicle-stimulating hormone (FSH) and luteinizing hormone (LH). These hormones induce various processes within the ovary, including follicular development, oocyte maturation and cumulus expansion, culminating in ovulation (Richards and Pangas, 2010). Prostaglandins (PGs) are considered to be the most important mediators involved in female reproductive processes (Algire et al., 1992; Chandras et al., 2004; Murdoch et al., 1986; Nuttinck et al., 2002), since LH surge induces the expression of prostaglandin-endoperoxide synthase 2 (Ptgs2, also known as cyclooxygenase-2), a rate-limiting enzyme of PG synthesis in the ovarian follicles (Duffy and Stouffer, 2001; Evans et al., 1983; Joyce et al., 2001; Sirois, 1994; Sirois and Dore, 1997; Sirois et al., 1992), and Ptgs2-deficient mice are mostly infertile because of severely impaired ovulation (Davis et al., 1999; Lim et al., 1997). Furthermore, non-steroidal anti-inflammatory drugs (NSAIDs) such as aspirin and indomethacin have been reported to inhibit ovulation in various species including humans (Barbosa

Abbreviations: ArKO, aromatase gene knockout; Est, estrogen sulfotransferase; E2, 17β-estradiol; FSH, follicle-stimulating hormone; hCG, human chorionic gonadotropin; Hpgd, NAD^+-dependent 15-hydroxyprostaglandin dehydrogenase; IU, international unit; LH, luteinizing hormone; PMSG, pregnant mare serum gonadotropin; PG, prostaglandin; Pges, PGE synthase; Pla2g4a, phospholipase A2, group IVA (cytosolic calcium-dependent); Ptgs2, prostaglandin-endoperoxide synthase 2; RT-QPCR, real-time quantitative PCR; TBST, Tris-buffered saline containing 0.1% Tween 20; WT, wild type.

* Corresponding author. Tel./fax: +81 88 880 2316.
E-mail address: todak@kochi-u.ac.jp (K. Toda).

0303-7207/$ - see front matter © 2012 Elsevier Ireland Ltd. All rights reserved.
http://dx.doi.org/10.1016/j.mce.2012.06.006